

# The Reaction-Diffusion Front for $A + B \rightarrow \emptyset$ in One Dimension.

G.T. Barkema

*Institute for Advanced Study, Olden Lane, Princeton, NJ 08540, USA.*

M.J. Howard and J.L. Cardy

*Department of Physics, Theoretical Physics, University of Oxford,*

*1 Keble Road, Oxford, OX1 3NP, United Kingdom.*

## Abstract

We study theoretically and numerically the steady state diffusion controlled reaction  $A + B \rightarrow \emptyset$ , where currents  $J$  of  $A$  and  $B$  particles are applied at opposite boundaries. For a reaction rate  $\lambda$ , and equal diffusion constants  $D$ , we find that when  $\lambda J^{-1/2} D^{-1/2} \ll 1$  the reaction front is well described by mean field theory. However, for  $\lambda J^{-1/2} D^{-1/2} \gg 1$ , the front acquires a Gaussian profile - a result of noise induced wandering of the reaction front center. We make a theoretical prediction for this profile which is in good agreement with simulation. Finally, we investigate the intrinsic (non-wandering) front width and find results consistent with scaling and field theoretic predictions.

Recently there has been considerable interest in the properties of diffusion limited chemical reactions [1,2]. Processes such as  $A + B \rightarrow \emptyset$ , where diffusing chemicals react irreversibly are believed to have many applications in physical, chemical, and biological systems. Particular attention has been paid to cases where a reaction front is formed between regions dominated by  $A$  or  $B$  particles. Such a situation can arise in the case where the two species are initially entirely segregated [3–10], or alternatively, and more simply, in a steady state situation, where  $A$  and  $B$  particles are injected at equal rates at opposite boundaries [9,11–13]. In this letter we study the latter model, in the case of equal diffusion constants  $D$  for the two species. The simplest description of these systems is provided by the inhomogeneous mean-field rate equations for the particle densities  $a$  and  $b$ , where it is assumed that the reaction rate  $R = \lambda ab$ :

$$\frac{\partial a}{\partial t} = D\nabla^2 a - \lambda ab \quad (1)$$

$$\frac{\partial b}{\partial t} = D\nabla^2 b - \lambda ab. \quad (2)$$

These equations predict a reaction front width which scales as  $w_{mf} \sim (\lambda J/D^2)^{-1/3}$ , where  $J$  are the (equal) imposed currents of  $A$  and  $B$  particles at the boundaries. However, it is well known that below a critical spatial dimension  $d_c = 2$  [9,12,13] microscopic density fluctuations become relevant, and as a result the mean field approach breaks down. For  $d = 1$  Cornell and Droz [12] have suggested that the fluctuations modify the scaling of the width to  $w \sim (J/D)^{-1/2}$ . Numerical simulations [10,12] have broadly confirmed these conclusions. However, there has been recent controversy in the time dependent version of the model, with initially separated reactants, over the existence of multiscaling in the spatial moments of the one dimensional reaction front [8,10]. More recent simulations by Cornell [10] have also indicated that the one dimensional profile is accurately described by a Gaussian. Hitherto this result has not been understood.

Theoretical approaches to understanding the crucial role played by fluctuations have centered on mappings of the microscopic dynamics of the reaction-diffusion system onto a quantum field theory [9,13,14]. This has allowed the effects of fluctuations to be sys-

tematically included by summing sets of Feynman diagrams. Renormalization group (RG) techniques have then been employed to form a perturbation expansion in  $\epsilon = 2 - d$ . These calculations have confirmed the modified scaling in  $d = 1$ , as well as pointing to the existence of power law tails, both in the densities and in the reaction front:

$$R = AD(J/D)^{\frac{19}{12}}|x|^{(9-7\epsilon)/12} \exp\left(-B(J/D)^{\frac{1}{2}}|x|^{(3-\epsilon)/2}\right) + CD^2 J^{-1}|x|^{-7+2\epsilon} + \dots \quad (3)$$

Here  $A, B, C$  are universal dimension dependent constants. One consequence of the power law tails is that sufficiently high order spatial moments of an evolving time dependent reaction front (with initially segregated reactants) should exhibit multiscaling. These results were derived on the basis of a finite reaction rate, which under the RG was found to flow to a universal  $O(\epsilon)$  fixed point. However, previous simulations of one dimensional reaction-diffusion systems have employed an infinite reaction rate, which enforces complete segregation between the two species. Furthermore only single occupancy of a given lattice site has previously been permitted. In this letter, we relax these restrictions by simulating a system with both multiple site occupancy and an adjustable, finite, reaction rate  $\lambda$ . This model is closer to that used in the analytic RG calculations.

Our model consists of a one dimensional lattice with  $L$  sites, on which particles of types  $A$  and  $B$  are located. In addition to this the model features reservoirs containing either  $A$  or  $B$  particles. The total number of particles of each species was set equal:  $N_A = N_B = N/2$ . Three distinct processes take place:

(1)  $A$  and  $B$  particles located on the lattice hop to neighboring sites in each direction with a hopping rate  $h$ , which we set equal to 1 (corresponding to  $D = 1$  in the continuum theory).

(2) Each  $A$  particle can react with each  $B$  particle on the same lattice site, with a reaction rate  $\lambda$ . After each reaction both particles are removed from the lattice and placed in their respective reservoirs.

(3) Each  $A$  ( $B$ ) particle in the reservoir is inserted onto the leftmost (rightmost) site in

the lattice with an insertion rate  $i$ . Clearly  $J = N_{res} \cdot i$ , where  $N_{res}$  is the number of particles in the reservoir. The purpose of these reservoirs is to break up correlations between particle annihilation inside the reaction front and particle reinsertion at the boundaries - the larger the reservoirs the smaller the correlations. The same effect can be achieved by increasing the system size, but this is computationally far less efficient, as in that case particles have to hop large distances before they can reach the reaction zone.

We carry out the simulations with rare-event dynamics (RED). In this approach no fixed time increment is present. First, in a specific configuration, a list is made of all the distinct events that might change the state of the system:  $4L - 2$  events for  $A$  and  $B$  particle hops,  $L$  events for recombination of a pair, and 2 events for insertion of a particle of either type; altogether  $5L$  events. For each event  $e_i$ , a rate  $r_i$  is calculated. Each step in the RED simulation now consists of incrementing the time scale with  $\Delta t = 1/\sum_j(r_j)$ , and then allowing selection (and execution) of an event. The probability that event  $e_i$  is chosen is equal to  $p_i = r_i/\sum_j(r_j)$ .

For an efficient implementation, a binary tree of events is constructed, where each branch contains one event and has a weight equal to the rate of that event. The weight of a parent node is equal to the sum of the weights of its children. As the root node contains the sum of all rates, the time increment  $\Delta t$  is easily obtained. For the selection of a particular event  $e_i$  with rate  $r_i$ , we start in the root node, descend to one of its children with a probability proportional to its weight, and iterate. The selected event is then executed and the tree is updated.

The initial configuration for each simulation consisted of linear density profiles for the  $A$  and  $B$  particles, which decreased from the left and the right hand edges to the system center. In all our simulations, we chose  $L$  such that no  $A$  particle ever penetrated the  $B$ -rich region to within 10 sites of the lattice boundary, and vice versa. Correlation and thermalization times varied with  $J$ ,  $N$ ,  $\lambda$  and  $L$ , and the tails of the reaction front required more thermalization than the middle section. The necessary thermalization time never exceeded  $10^7$  events. To be safe, we thermalized our system in all runs over  $10^8$  events.

We consider first the regime  $\lambda J^{-1/2} D^{-1/2} \ll 1$ , where the mean field reaction front width  $w_{mf} \sim (\lambda J/D^2)^{-1/3}$  is much larger than the predicted fluctuation modified width  $\sim (J/D)^{-1/2}$ . In this case we expect that the behavior of the system should be close to mean field. Solving equations (1) and (2) for  $a$  and  $b$ , we find that the mean field reaction front  $R_{mf} = \lambda ab$  has the form  $R_{mf} = J(\lambda J/D^2)^{1/3} S([\lambda J/D^2]^{1/3} x)$ , where asymptotically (for  $(\lambda J/D^2)^{1/3} |x| \gg 1$ ) we have

$$S \sim ([\lambda J/D^2]^{1/3} |x|)^{\frac{3}{4}} \exp\left(-\frac{2}{3}([\lambda J/D^2]^{1/3} |x|)^{\frac{3}{2}}\right) \quad (4)$$

Hence the mean-field solution predicts that measured data for the reaction front should collapse if  $R/[J(\lambda J/D^2)^{1/3}]$  is plotted as a function of  $(\lambda J/D^2)^{1/3} x$ , as shown in figure 2. In this case the number of particles  $N$  (which varied from between 1300 to 12000) was tuned to obtain the desired  $J$ .

The collapsed data is in good agreement with the mean field prediction, although there is a slight tendency for our simulation data to lie to the right of  $R_{mf}$ , for the largest values of  $(\lambda J/D^2)^{1/3} x$ . In this region, where the number of minority particles is small, we expect that noise from the reaction front will again become important, leading to a widening of the profile. Note that these simulation results were found not to depend on the inclusion of reservoirs in our model, implying that the existence of correlations between particle annihilation and reinjection was unimportant in this case.

In the limit  $\lambda J^{-1/2} D^{-1/2} \gg 1$  the mean field solution predicts that the reaction front will become increasingly narrow. However, the simulations disagree with this assertion - the reaction front keeps a finite width even if  $\lambda$  is made very large. Our analysis, described below, distinguishes two components of this width: one is intrinsic, and the other is caused by the ability of the center of the front to wander. The intrinsic width is calculable using the RG approach already outlined, whereas the front wandering can be understood by considering the fluctuations in the field  $\psi = a - b$ , whose zero may be taken as defining the center of the front. Including the effects of reaction front noise (which is relevant in one dimension), the field theory [13] leads to the following equation for  $\psi$ :

$$\frac{\partial \psi}{\partial t} = D \nabla^2 \psi + \eta. \quad (5)$$

Here  $\eta$  is the reaction front noise, satisfying  $\langle \eta \rangle = 0$  and

$$\langle \eta(x, t) \eta(x', t') \rangle = 2\delta(t - t')\delta(x - x')R, \quad (6)$$

where the reaction rate at the wandering front, with width  $w_g$ , has the form  $R = (J/w_g)S(x/w_g)$ . It is important to realize that, while  $\psi$  is on average equal to  $\langle a \rangle - \langle b \rangle$ , its fluctuations are *not* the same as those in the density difference. This arises from the non-trivial commutation properties of the operators within the field theory. More details on this point (within the context of an  $A + A \rightarrow \emptyset$  reaction) can be found in [14]. This fact accounts for the non-conservative nature of the noise in equation (5). We may now decompose  $\psi$  into its mean field part together with higher order Fourier harmonics:

$$\psi = -(J/D)x + \sum_{n=0} \chi_n(t) \cos\left(\frac{(2n+1)\pi x}{L}\right) \quad (7)$$

for  $-(L/2) \leq x \leq (L/2)$ . These corrections are the most general possible which both couple to the noise (i.e. the harmonics have a non-zero amplitude at  $x = 0$ ), and which are appropriate for the non-conservative nature of the noise. Furthermore the densities on the boundaries are kept constant by these additional terms. We can now insert the above expression into the noisy diffusion equation and Fourier expand the reaction front noise (which is concentrated near  $x = 0$ ). In the large time limit we find

$$\chi_n(t) \approx \frac{2\sqrt{2J}}{L} \int_0^t \eta(t') \exp\left[\frac{(2n+1)^2\pi^2 D}{L^2}(t' - t)\right] dt', \quad (8)$$

where now

$$\langle \eta(t) \rangle = 0, \quad \langle \eta(t) \eta(t') \rangle = \delta(t - t'). \quad (9)$$

Clearly  $\psi(x = 0, t) = \sum \chi_n(t)$  is a Gaussian random variable with

$$\langle \psi(0, t)^2 \rangle - \langle \psi(0, t) \rangle^2 = \sum_{n,m} \langle \chi_n(t) \chi_m(t) \rangle \quad (10)$$

$$\sim \frac{J}{\pi D} \ln\left(\frac{cL}{w_g}\right), \quad (11)$$

in the large time limit, with  $c$  a constant, and where the upper limit is provided by the finite width  $w_g$  of the wandering reaction front. Assuming that the fluctuations of  $\psi$  are small in comparison with the system size, then the gradient of  $\psi$  at  $x = 0$  remains approximately equal to  $-(J/D)$ . Hence to leading order we expect the position of the zero of the  $\psi$  field to be a Gaussian random variable with width  $w_g$ , given by the recursive relation:

$$w_g = \left[ \frac{\ln(cL/w_g)}{\pi(J/D)} \right]^{\frac{1}{2}}. \quad (12)$$

From our simulation data (in the limit  $\lambda J^{-1/2} D^{-1/2} \gg 1$ ) we have plotted  $Rw_g/J$  as a function of  $x/w_g$ , where in (12) we used  $c = 0.5$  (see figure 3). The collapsed data is well described by a normalized Gaussian, with width 1, in good agreement with our theory. This indicates that the higher order non-Gaussian corrections to the distribution of the zero of the  $\psi$  field are indeed small. Note that the logarithmic factor in (12) is essential for a good fit to the data.

We can clearly see from figure 3 that the wandering Gaussian dominates over the intrinsic profile to form the overwhelming component of the front. Notice also that we find a basic  $(J/D)^{-1/2}$  scaling, in agreement with earlier predictions [9,12,13]. Previously, however, only the *intrinsic* part of the front was being analyzed, whereas we have been studying the *wandering* piece. The scaling agreement is simply a consequence of dimensional analysis - any quantity with the dimensions of length, which is independent of  $\lambda$ , must scale as  $(J/D)^{-1/2}$ . We may also generalize our calculation to the time dependent case, where a reaction front is formed quasistatically between initially entirely segregated reactants. In this situation we find  $w_g \sim t^\alpha (\ln t)^{1/2}$ , where  $\alpha = 1/4$ . The presence of the logarithm may explain the slow convergence found in measurements of the exponent  $\alpha$  [10].

If we wish to study the intrinsic component of the front in the non-mean field limit ( $\lambda J^{-1/2} D^{-1/2} \gg 1$ ), we must now find a way of suppressing the dominance of the wandering Gaussian part. One way in which this can be achieved is to measure the reaction rate  $R_r$  as a function of  $|x - x_p|$ , the distance between successive reaction events at  $x_p$  and  $x$ . This enables the intrinsic profile to be studied, as the front center has little time to move on such

short time scales. These reaction events are effectively uncorrelated, so that the relative reaction rate  $R_r$  is given by

$$R_r(\tilde{x}) = \int R(x)P(x_p)\delta(x - x_p - \tilde{x})dx dx_p, \quad (13)$$

where  $P(x_p)dx_p = R(x_p)dx_p / \int R(x_p)dx_p$  is the probability that the previous reaction occurred between  $x_p$  and  $x_p + dx_p$ . In our simulations of  $R_r$  we kept the insertion rate  $i$  small, and hence many particles were present in the reservoirs. We were therefore able to effectively simulate a much bigger system, with a large number of particles. This ensured that correlations between annihilation and reinsertion, which would otherwise have modified the intrinsic profile, were kept to a minimum. Our simulation data is shown in figure 4, which shows a convincing data collapse of  $R_r(J/D)^{-1/2}/J$  plotted against  $|x - x_p|(J/D)^{1/2}$ . As we are now studying the intrinsic profile, this result finally confirms the scaling predictions of [9,12,13]. For large values of  $|x - x_p|(J/D)^{1/2}$  we also find a tail which is consistent with the RG improved tree level prediction  $\log(R) \sim -B(J/D)^{1/2}|x|$  (implying  $\log(R_r) \sim -B(J/D)^{1/2}|\tilde{x}|$ ). Our data provides no clear indication of the power law tails predicted in [13]. However, such tails would be very hard to see in measurements of the relative reaction rate  $R_r$ , as the power law exponent would be large ( $7 - 2\epsilon + O(\epsilon^2)$ ). Simulations have also been performed in the mean field regime. In this case  $R_r/[J(\lambda J/D^2)^{1/3}]$  was found to collapse when plotted against small values of  $(\lambda J/D^2)^{1/3}|x - x_p|$ . However, for larger values, the collapse no longer worked well, probably due to the increased importance of fluctuations in the asymptotic regime.

In summary, our ability to adjust the reaction rate has enabled us to find two regimes for the  $A + B \rightarrow \emptyset$  front in one dimension. For  $\lambda J^{-1/2}D^{-1/2} \ll 1$  mean field predictions work well, whereas for  $\lambda J^{-1/2}D^{-1/2} \gg 1$  the front is dominated by a Gaussian profile, a result of fluctuation induced wandering. Our theoretical prediction for this shape agrees well with simulations. Finally, we have succeeded in studying the intrinsic profile, where the shape and scaling properties match previous RG calculations.

The authors thank S. Cornell and M. Droz for useful discussions. We acknowledge



financial support from the EPSRC, under Grant No. GR/J78044 (GTB and JLC).

## REFERENCES

- [1] V. Kuzovkov and E. Kotomin, Rep. Prog. Phys. **51**, 1479 (1988).
- [2] A.A. Ovchinnikov, S.F. Timashev, and A.A. Belyy, *Kinetics of Diffusion Controlled Chemical Processes* (Nova Science Publishers, New York, 1990).
- [3] L. Gálfi and Z. Rácz, Phys. Rev. A **38**, 3151 (1988).
- [4] H. Taitelbaum, S. Havlin, J. Kiefer, B. Trus, and G. Weiss, J. Stat. Phys. **65**, 873 (1991).
- [5] S. Cornell, M. Droz, and B. Chopard, Phys. Rev. A **44**, 4826 (1991).
- [6] H. Larralde, M. Araujo, S. Havlin, and H.E. Stanley, Phys. Rev. A **46**, 855 (1992).
- [7] H. Larralde, M. Araujo, S. Havlin, and H.E. Stanley, Phys. Rev. A **46**, R6121 (1992).
- [8] M. Araujo, H. Larralde, S. Havlin, and H.E. Stanley, Phys. Rev. Lett. **71**, 3592 (1993); Phys. Rev. Lett. **75**, 2251 (1995).
- [9] B.P. Lee and J. Cardy, Phys. Rev. E **50**, R3287 (1994).
- [10] S. Cornell, Phys. Rev. E **51**, 4055 (1995).
- [11] E. Ben-Naim and S. Redner, J. Phys. A **25**, L575 (1992).
- [12] S. Cornell and M. Droz, Phys. Rev. Lett. **70**, 3824 (1993); S. Cornell, Phys. Rev. Lett. **75**, 2250 (1995).
- [13] M. Howard and J. Cardy, J. Phys. A **28**, 3599 (1995).
- [14] B.P. Lee, J. Phys. A **27**, 2633 (1994).

## FIGURES

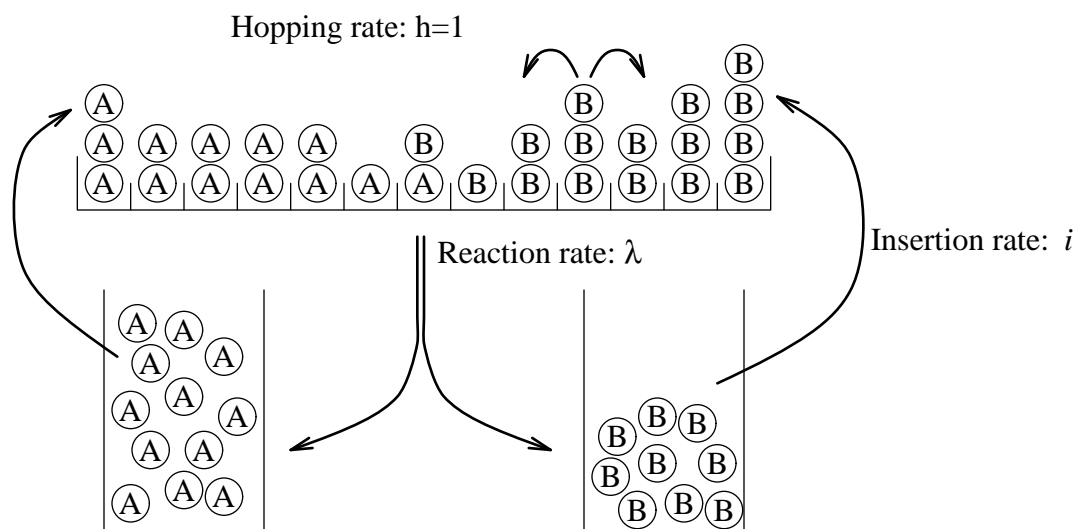
FIG. 1. In our model,  $A$  and  $B$  particles are located on a one-dimensional lattice. Three processes occur: particles can hop one lattice site to the left or right with rate  $h = 1$ ; each pair of  $A$  and  $B$  particles at the same site can react with a rate  $\lambda$ , after which they are moved to their respective reservoirs; and  $A$  ( $B$ ) particles enter the lattice on the left (right) sides with an insertion rate  $i$ .

FIG. 2. Collapsed data in the regime  $\lambda J^{-1/2} D^{-1/2} \ll 1$ . Solid line: mean field prediction. Squares: simulation results for runs over  $10^9$  events and  $i = 1000$ , with  $D = 1$ ,  $\lambda = 0.001, 0.01, 0.1$ , and  $J = 0.1, 0.2, 0.5, 1.0$ .

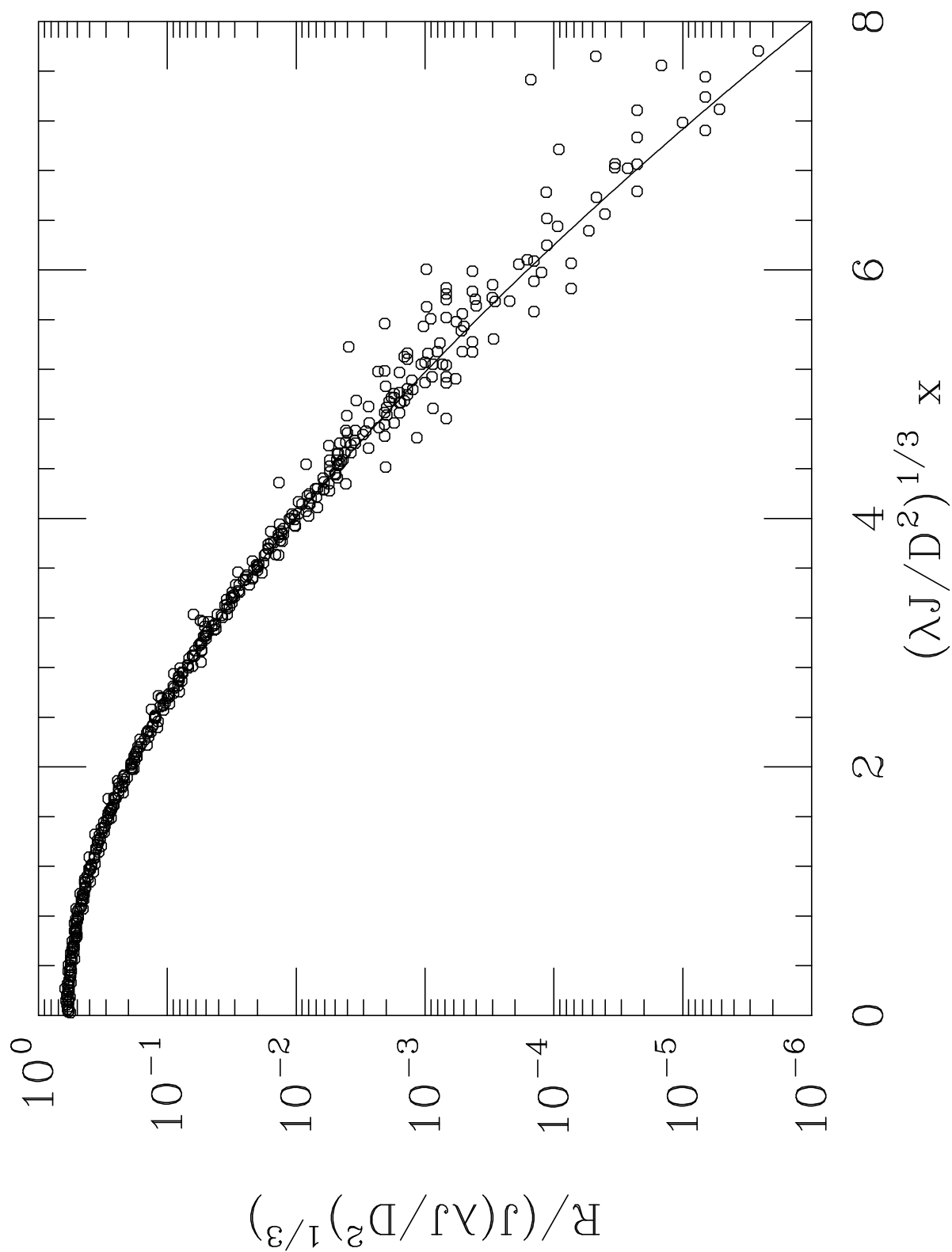
FIG. 3. Collapsed data in the regime  $\lambda J^{-1/2} D^{-1/2} \gg 1$ . Solid line: normalized Gaussian; Data points: simulation results over  $10^9$  events with  $D = 1$ ,  $\lambda = 1000$ ,  $i = 1000$ ,  $J = 0.1, 0.2, 0.5, 1.0$ , and  $N = 100$  (0),  $1000$  (+).

FIG. 4. Collapsed data for the relative reaction rate in the regime  $\lambda J^{-1/2} D^{-1/2} \gg 1$ . Simulations were for  $10^{10}$  events, with  $D = 1$ ,  $N = 200, 1100, 10100$ .

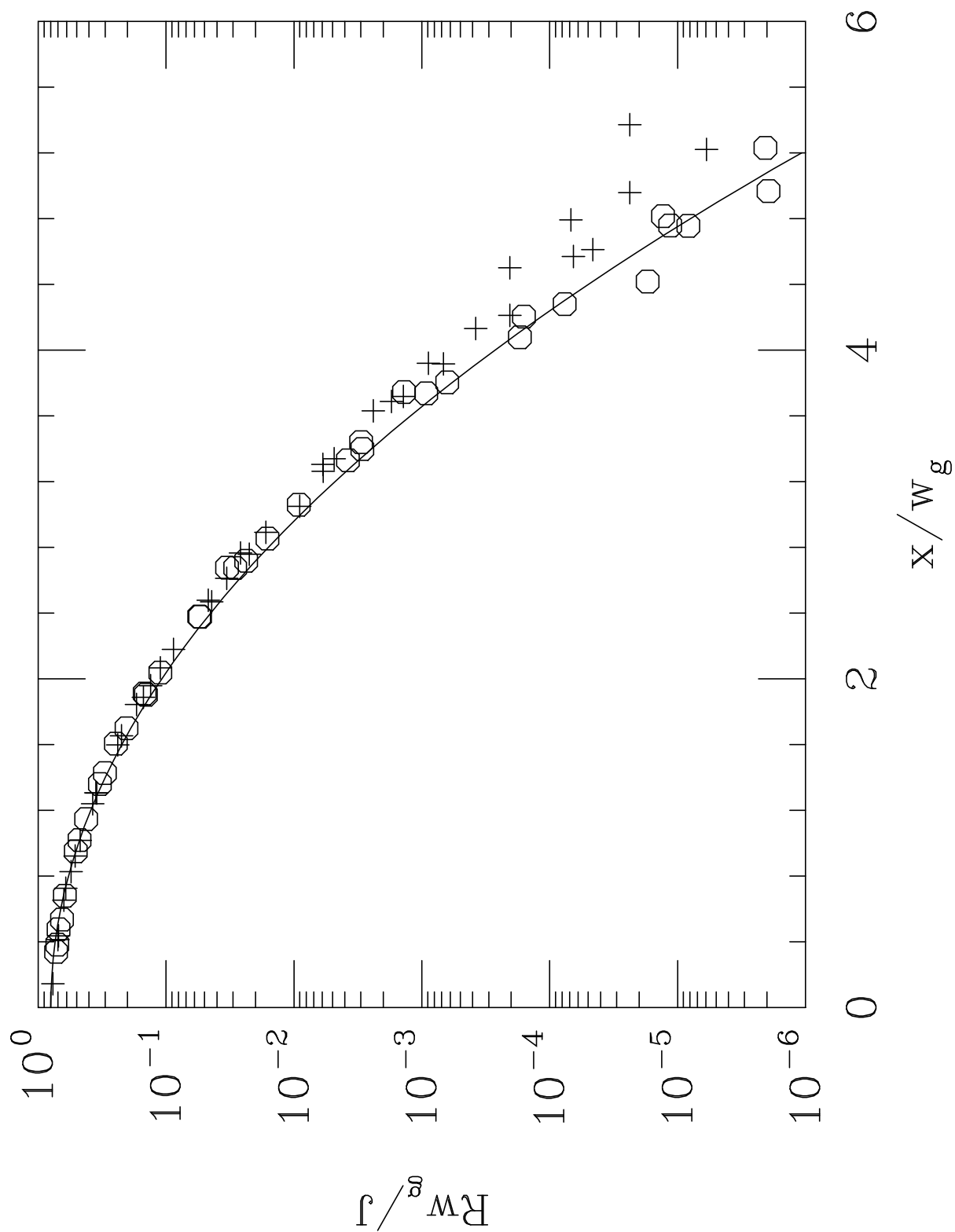
# Barkema/Howard/Cardy Fig. 1



Barkema/Howard/Cardy Fig. 2



Barkema/Howard/Cardy Fig. 3



Barkema/Howard/Cardy Fig. 4

